HHS Public Access

Author manuscript

Immunohorizons. Author manuscript; available in PMC 2021 June 03.

Published in final edited form as:

Immunohorizons. ; 5(4): 193–209. doi:10.4049/immunohorizons.2100018.

Indole-3-Carbinol-Dependent Aryl Hydrocarbon Receptor Signaling Attenuates the Inflammatory Response in Experimental Necrotizing Enterocolitis

Lila S. Nolan[*], **Belgacem Mihi**[*], **Pranjal Agrawal**[†], **Qingqing Gong**[*], **Jamie M. Rimer**[*], **Shay S. Bidani**[*], **Sarah E. Gale**[*], **Martin Goree**[*], **Elise Hu**[*], **Wyatt E. Lanik**[*], **Elizabeth Huang**[*], **Jennifer K. Bando**[‡], **Victoria Liu**[†], **Angela N. Lewis**[*], **Aiza Bustos**[†], **Zerina Hodzic**[§], **Marie L. Laury**[¶], **Misty Good**[*]

[*]Division of Newborn Medicine, Washington University School of Medicine, St. Louis, MO;

[†]Washington University in St. Louis, St. Louis, MO;

[‡]Department of Pathology and Immunology, Washington University School of Medicine, St. Louis, MO;

[§]Department of Medicine, University of Pittsburgh Medical Center, Pittsburgh, PA;

[¶]Genome Technology Access Center, McDonnell Genome Institute, Washington University School of Medicine, St. Louis, MO

Abstract

Necrotizing enterocolitis (NEC) causes significant morbidity and mortality in premature infants; therefore, the identification of therapeutic and preventative strategies against NEC remains a high priority. The ligand-dependent transcription factor aryl hydrocarbon receptor (AhR) is well known to contribute to the regulation of intestinal microbial communities and amelioration of intestinal inflammation. However, the role of AhR signaling in NEC is unclear. Experimental NEC was induced in 4-d-old wild-type mice or mice lacking AhR expression in the intestinal epithelial cells or AhR expression in $CD11c^+$ cells ($AhR^{\Delta CD11c}$) by subjecting animals to twice daily hypoxic stress and gavage feeding with formula supplemented with LPS and enteric bacteria. During NEC, compared with wild-type mice treated with vehicle, littermates treated with an AhR proligand, indole-3-carbinol, had reduced expression of *Il1b* and *Marco*, a scavenger receptor that mediates dendritic cell activation and the recognition and clearance of bacterial pathogens by macrophages. Furthermore, indole-3-carbinol treatment led to the downregulation of genes involved in cytokine and chemokine, as revealed by pathway enrichment analysis. AhR expression in the intestinal epithelial cells and their cre-negative mouse littermates were similarly susceptible to experimental NEC, whereas $AhR^{\Delta CD11c}$ mice with NEC exhibited heightened inflammatory responses

Address correspondence and reprint requests to: Dr. Misty Good, Division of Newborn Medicine, Department of Pediatrics, Washington University School of Medicine, St. Louis Children's Hospital, 660 South Euclid Avenue, Campus Box 8208, St. Louis, MO 63110. mistygood@wustl.edu.

The sequences presented in this article have been submitted to the Gene Expression Omnibus (https://www.ncbi.nlm.nih.gov/geo/) under accession number GSE154617.

The online version of this article contains supplemental material.

compared with their cre-negative mouse littermates. In seeking to determine the mechanisms involved in this increased inflammatory response, we identified the Tim-4^{-} monocyte-dependent subset of macrophages as increased in AhR$^{\Delta CD11c}$ mice compared with their cre-negative littermates. Taken together, these findings demonstrate the potential for AhR ligands as a novel immunotherapeutic approach to the management of this devastating disease.

INTRODUCTION

Intricate factors regulate the balance between immunity and tolerance of commensal microbes involved in intestinal homeostasis. The neonatal intestine relies on epithelial barrier integrity and function to provide host defense against harmful stimuli (1). An insufficient intestinal barrier, immature immune system, and dysbiotic microbiome during the neonatal period predispose premature infants to necrotizing enterocolitis (NEC), a devastating disease (1–3). Widespread intestinal inflammation, leading to necrosis, perforation, and death, is commonly seen in NEC (2, 4). However, the mechanistic pathways or cell types involved in the exaggerated intestinal inflammation during NEC are not entirely understood.

Although the activation of aryl hydrocarbon receptor (AhR) signaling has a prominent role in intestinal homeostasis, its role during NEC is not well understood (5–7). Upon binding AhR ligands, AhR translocates from the cytoplasm to the nucleus, where it activates gene transcription and impacts a broad range of processes including cell growth and differentiation and oncogenesis (8). Agonistic AhR ligands have important functional roles in various tissue systems and organs and can regulate the inflammatory response (7, 9–11). Prior studies have implicated AhR ligands in promoting epithelial barrier integrity and modulating the inflammatory response in adult mouse models of colitis (10, 12–14). Despite extensive studies in adult mouse models, the role of AhR ligands during NEC-induced inflammation remains unknown.

Natural AhR ligands are derived from exogenous dietary in-take or endogenous tryptophan catabolism by the gut microbiota (15, 16). Dietary AhR proligands such as indole-3-carbinol (I3C) are derived from cruciferous vegetables, such as cabbage, cauliflower, and broccoli (5, 17, 18). I3C undergoes gastric conversion by acid hydrolysis to high-affinity ligands and, thereby, constitutes an important source of exogenous dietary AhR proligands absorbed by the gastrointestinal tract (19). Dietary supplementation with I3C protects against murine intestinal inflammation and colorectal cancer in models of tumorigenesis (20). Although several protective strategies against NEC have been identified, including an exclusive human breast milk diet, a definitive therapeutic target that can reverse the aggressive disease process has not been discovered (21–23). Therefore, we aimed to investigate the role of a dietary AhR proligand on intestinal immunity and the inflammatory response during neonatal experimental NEC and determine the cellular mechanisms that mediate this response.

MATERIALS AND METHODS

Study approvals

Human.—Human fetal small intestines were obtained from elective or spontaneous terminations at fewer than 24 wk of gestation from the University of Pittsburgh Health Sciences Tissue Bank at Magee-Womens Hospital. All discarded tissue was obtained and processed in accordance with anatomical tissue procurement guidelines with a waiver of consent after approval from the University of Pittsburgh Institutional Review Board.

Mice.—All animal experiments were performed in an American Association for the Accreditation of Laboratory Animal Care-accredited and specific pathogen–free animal facility at the Washington University School of Medicine in St. Louis. All mice were bred, maintained, and housed in accordance with the procedures outlined in the Guide for the Care and Use of Laboratory Animals under a study proposal approved by the Institutional Animal Care and Use Committee (protocol no. 20190190) of the Washington University School of Medicine in St. Louis.

C57BL/6 mice were obtained from The Jackson Laboratory (stock no. 000664). To generate mice lacking AhR expression in intestinal epithelial cells ($AhR^{\Delta IEC}$), AhR flox/flox mice (stock no. 006203; The Jackson Laboratory) were crossed with villin-cre mice (stock no. 021504; The Jackson Laboratory). To generate mice lacking AhR in dendritic cells ($AhR^{\Delta CD11c}$), AhR flox/flox mice were crossed with CD11c-cre mice (stock no. 008068; The Jackson Laboratory). Both mouse lines bred normally, and cre-positive offspring showed no distinction in viability or baseline health in comparison with cre-negative littermates.

Induction of experimental NEC in mouse pups

NEC was induced in neonatal mice using a model of hypoxic stress and infant formula supplemented with LPS and enteric bacteria (Supplemental Fig. 1). Four-day-old mice were randomly assigned to experimental groups, and pups either remained with the mother or were separated from the dams and placed in a new cage maintained at 37°C in an infant incubator. Experimental NEC was induced in pups by gavage feeding a formula mixture containing Similac Advance Optigro with Iron infant formula (Abbott Nutrition) and Esbilac canine milk replacer (ratio 2:1). The formula was prepared daily and inoculated with enteric bacteria cultured from a human infant with NEC totalis, the most severe form of NEC (24). The aliquot of enteric bacteria was obtained from a frozen bacterial glycerol stock and prepared daily in an overnight culture with auto-claved Luria–Bertani broth culture medium (Λ Biotech). LPS (Sigma-Aldrich) at a concentration of 2.5 μg/g average body weight was added to the formula.

A 1.9 French Single-Lumen Silicon Peripherally Inserted Central Catheter was used for oral gavage of the pups with slow infusion of 80 μl of formula. Feedings were provided six times daily, and following two feeds per day, the pups were subjected to 10 min of hypoxic stress in a hypoxia chamber (Billups-Rothenberg) containing 95% nitrogen and 5% oxygen. After

72 h of the model, pups were euthanized in accordance with Institutional Animal Care and Use Committee policy. The terminal segment of the ileum was resected for further analysis.

I3C supplementation

Where indicated, a subset of pups from the breastfed and formula-fed groups were designated to receive AhR proligand I3C (Sigma Life Sciences) supplementation daily, starting at the on-set of the NEC model (Supplemental Fig. 1A). I3C dosing was established based on prior investigations of dose efficacy and toxicity in rodents (25, 26). The I3C formulation was prepared each morning at a concentration of 50 μg/g body weight using the daily average weight of the pups. The I3C was then homogenized in corn oil (Sigma Life Sciences) using a sonicator (Thermo Fisher Scientific), and 30 μl of the I3C solution was administered to pups twice daily by oral gavage. Breastfed and formula-fed pups that did not receive I3C instead received the vehicle corn oil (30 μl) twice daily via oral gavage.

Histological assessment

Segments of resected terminal ilea were processed by the Digestive Disease Research Core Center at the Washington University School of Medicine in St. Louis. Formalin-fixed, paraffin-embedded ileal sections were stained with H&E. Images of stained tissue sections were taken with a Zeiss AxioScan .Z1 with a 20× objective (ZEISS). Using ImageJ software, the disease severity was assessed in a blinded fashion based on the extent of histological lesions. Normal tissue sections were characterized by intact villi. Mild lesions were characterized by areas with villi blunting, as reflected by a substantial reduction of the villi length. Severe lesions were defined as areas with a complete lack of villi structure. The data were reported as the percentage of lesion extent from the total length of the histological specimen.

Quantitative real-time PCR

RNA extraction from resected intestinal tissue stored in RNA Later (Invitrogen) was carried out with TRIzol (Thermo Fisher Scientific) per the manufacturer's instructions. Chloroform was added to the samples prior to centrifugation. The top aqueous layer was isolated, to which isopropanol and glycogen were added. The samples were permitted an incubation period and additional centrifugation for RNA precipitation. The supernatant was discarded, and the remaining RNA pellet was washed with 70% ethanol. Samples underwent additional centrifugation and supernatant removal to permit drying of the RNA pellet prior to adding 50 μl RNase-free water. RNA purity was confirmed with a NanoDrop Spectrophotometer. RNA was retro-transcribed using the QuantiTech Reverse Transcription Kit (QIAGEN) according to the manufacturer's instructions. Quantitative real-time PCR (qRT-PCR) was performed using IQ SYBR Green Supermix and the CFX Connect Real-Time PCR Detection System (Bio-Rad Laboratories). The primers are listed in Table I, and a melting curve was added to the amplification protocol to ensure the absence of primer dimer formation or multiple amplicons. The expression of genes assessed by qRT-PCR was quantified relative to the housekeeping gene *RPLO*. A V-plex immunoassay (Meso Scale Diagnostics) was performed by the Immunomonitoring Laboratory at Washington University for IL-1β protein quantification.

RNA sequencing and analysis

Bulk RNA sequencing (RNA-seq) was performed on terminal ilea by the Genome Technology Access Center at the Washington University School of Medicine in St. Louis. Total RNA was isolated using TRIzol. RNA samples with an RNA integrity number of at least 7 were used to generate libraries by Genome Technology Access Center using the RNA zero kit (Roche Diagnostics). Samples were prepared according to the library kit manufacturer's protocol and were indexed, pooled, and sequenced on an Illumina HiSeq. Base calls and demultiplexing were performed with Illumina's bcl2fastq software and a custom python demultiplexing program with a maximum of one mismatch in the indexing read. To generate heat maps, mRNA expression was analyzed using Partek Flow software. Adapters were removed, and reads were aligned to the MM10 assembly with Bowtie 2 and quantified to Ensembl transcript release 99 with an average coverage of 10×. Reads were normalized to total counts per million. Features containing fewer than 10 reads were not included in the analysis.

For pathway analysis, RNA-seq reads were aligned to the Ensembl release 76 primary assembly with STAR version 2.5.1a (27). Gene counts were derived from the number of uniquely aligned unambiguous reads by Subread:featureCount version 1.4.6-p5 (28). Isoform expression of known Ensembl transcripts was estimated with Salmon version 0.8.2 (29). Sequencing performance was assessed for the total number of aligned reads, the total number of uniquely aligned reads, and features detected. The ribosomal fraction, known junction saturation, and read distribution over known gene models were quantified with RSeQC version 2.6.2 (30).

All gene counts were then imported into the R/Bioconductor package EdgeR (31), and trimmed mean of M values normalization size factors were calculated to adjust for sample differences in library size. Ribosomal genes and genes not expressed in the smallest group size minus one sample greater than one count-per-million were excluded from further analysis. The trimmed mean of M values size factors and the matrix of counts were then imported into the R/Bioconductor package Limma (32). Weighted likelihoods based on the observed mean-variance relationship of every gene and sample were then calculated for all samples with the voomWithQualityWeights (33). The performance of all genes was assessed with plots of the residual SD of every gene to their average log count with a robustly fitted trend line of the residuals. Differential expression analysis was then performed to analyze for differences between groups, and the results were filtered for only those genes with Benjamini–Hochberg false discovery rate–adjusted p values ≤0.05.

For each contrast extracted with Limma, global perturbations in known Gene Ontology terms, Molecular Signatures Database, and Kyoto Encyclopedia of Genes and Genomes (KEGG) pathways were detected using the R/Bioconductor package Generally Applicable Gene-set Enrichment for Pathway Analysis (34) to test for changes in expression of the reported log 2-fold changes reported by Limma in each term versus the background log 2-fold changes of all genes found outside the respective term. Perturbed KEGG pathways in which the observed log 2-fold changes of genes within the term were significantly perturbed in a single-direction versus background or in any direction compared with other genes

within a given term with p values ≤0.05 were rendered as annotated KEGG graphs with the R/Bioconductor package Pathview (35).

Lamina propria cell isolation and flow cytometry

Lamina propria cells were isolated from the last 5 cm of the distal small intestine. Briefly, intestinal specimens were opened longitudinally, washed in ice-cold PBS, and incubated in 2 mM EDTA (Corning)/PBS for 30 min at 4°C in an MACSmix tube rotator (Miltenyi Biotec). After transferring the tissue samples to ice-cold PBS, the epithelial cells were removed by pipetting three times up and down. The remaining intestinal tissues were digested in RPMI 1640 (Sigma-Aldrich) supplemented with 2.5% FBS, 1 mg/ml collagenase type 4 (Worthington-Biochem), and 0.05 mg/ml DNase (Sigma-Aldrich) at 4°C for 40 min in an orbital shaker. The digestion was quenched with RPMI 1640 supplemented with 10% FBS and passed successively through 70- and 40-μm strainers to obtain a single-cell suspension. After washing the cells in RPMI 1640 supplemented with 10% FBS, they were resuspended in PBS and stained with Zombie NIR Fixable Viability dye (BioLegend) following the manufacturer's instructions. After a washing step in FACS buffer (PBS supplemented with 3% FBS), the cells were sequentially stained on ice with CD16/CD32 Abs (Miltenyi Biotec) for 10 min and stained with the manufacturer's suggested concentration for anti-mouse PE-conjugated CD4 (BD Pharmingen), FITC-conjugated CD8 (eBioscience), PE-conjugated (BioLegend), or biotin-conjugated CD11b (eBioscience), BV421-conjugated (BD Horizon) or APC-conjugated CD11c (eBioscience), PerCP-Cy5.5–conjugated CD45 (eBioscience), BV421-conjugated CD64 (BioLegend), PE/Cy7-conjugated CD103 (BioLegend), FITC-conjugated MHC class II (BioLegend), and PE-conjugated Tim-4 (BioLegend) for 20 min. Intracellular staining for BV421-conjugated Foxp3 (BioLegend), BV421-conjugated IFN-γ (BD Horizon), FITC-conjugated IL-1β (eBioscience), and APC-conjugated IL-17A (eBioscience) was performed according to the eBioscience protocol. For experiments requiring $CD11c^+$ enrichment, isolated lamina propria cells were enriched using CD11c MicroBeads Ultrapure (Miltenyi Biotec) and MS Columns (Miltenyi Biotec) according to the manufacturer's instructions prior to Ab staining.

Small intestine epithelial isolation was accomplished using an established method (36). Briefly, small intestinal sections were transected longitudinally, washed in cold PBS, and incubated in PBS with 30 mM EDTA, 1.5 mM 1,4-DTT, and 10 μM Y27632 for 20 min at 4°C. The tissue was then transferred to a solution containing PBS with 30 mM EDTA and 10 μM Y27632 for 10 min at 37°C. The conical tube containing the tissue was forcefully shaken for 30 s for removal of the epithelium from the remnant intestinal tissue. The cells were washed in PBS with 10% FBS and resuspended in HBSS (Life Technologies) with 8 mg dispase (Corning) for 10 min at 37°C. The conical tube containing the sample was forcefully shaken intermittently during the incubation for cellular dissociation. Following the incubation, 10% FBS and 10 mg/ml DNase were added to the digestion, which was passed sequentially through 70- and 40-μm strainers to obtain a single-cell suspension. The cells were rinsed in HBSS with 10% FBS and resuspended in intestinal epithelial stem cell staining media containing DMEM: Nutrient Mixture F-12 (Sigma-Aldrich) with 15 mM HEPES (Life Technologies), 2 mM glutamine (Sigma-Aldrich), and 100 μg/ml penicillin/streptomycin (Life Technologies). Cells were stained with the manufacturer's recommended

concentration for anti-mouse FITC-conjugated CD45 (BioLegend), BV421-conjugated EpCAM (CD326) (BioLegend) and eFluor660-conjugated AhR (eBioscience).

Cell acquisition was carried out using MACSQuant Analyzer 10 (Miltenyi Biotec), and the data were analyzed with FlowJo software (Tree Star).

Statistical analysis

Statistical analyses with Mann–Whitney *U* tests, ANOVA, and two-tailed Student *t* tests were performed, where indicated using GraphPad Prism software version 8.0. Statistical significance was set at $p < 0.05$. All experiments were performed at least in triplicate.

RESULTS

AhR activation by I3C attenuates the inflammatory response during NEC

Previous studies have shown that in immature human cell lines and human-derived enteroids, the AhR ligand indole-3-lactic acid inhibits IL-8 secretion elicited by the proinflammatory cytokine IL-1β, supporting the hypothesis that AhR activation may ameliorate inflammation during NEC (37). Because NEC occurs most commonly in premature infants, we first analyzed *AhR* expression in premature intestine. *AhR* expression was seen as early as 17 wk of gestation in human fetal small intestine (Fig. 1A). We then analyzed *Ahr* expression in the small intestine of newborn mouse pups during development from birth to adulthood as defined by postnatal day-of-life (P)1–49. There was no significant difference in *Ahr* expression observed between P1–14 pups, the period in which our NEC model is conducted. There was a slight, but statistically significant, decrease in *Ahr* expression between P1 and P21, P28, and P49 pups (Fig. 1B). To assess the implication of these differences on AhR signaling, we analyzed the expression of *Cyp1a1*, a known direct target of AhR. In healthy wild-type mice, *Cyp1a1* expression in the terminal ileum is expressed during development (Fig. 1B), suggesting that other factors may be compensating for the decrease in *AhR* expression in later time points.

Having established *Ahr* and *Cyp1a1* expression during wild-type mouse development, we next evaluated the effect of I3C treatment on AhR activation in neonatal mice by evaluating small intestine mRNA expression of *Cyp1a1* as the downstream target of AhR signaling. As anticipated, I3C induced an AhR-dependent gene response in both healthy controls and wild-type mice subjected to NEC by producing a significant increase in *Cyp1a1* expression ($p < 0.0001$), indicating the activation of AhR signaling by enteral I3C (Fig. 1C). We then characterized the effect of AhR signaling in NEC through the assessment of enteral I3C supplementation on intestinal architecture. Induction of NEC resulted in marked destruction of the intestinal epithelium and loss and fragmentation of the villi (Fig. 1D). Histology scoring of stained tissue samples revealed that I3C supplementation improved the proportion of small intestine affected by mild NEC lesions ($p = 0.0017$) and increased the proportion of small intestine with no lesion ($p = 0.0004$) compared with animals treated with the vehicle corn oil (Fig. 1E). Taken together, these findings demonstrate that I3C-mediated AhR signaling supplementation protects the structural architecture of the intestinal epithelium during NEC.

Given the established role of AhR signaling in immune modulation and the protective effect of AhR activation on NEC pathology, we next analyzed the impact of I3C treatment on the proinflammatory cytokine response during NEC. The small intestine mRNA expression of *Il1b*, a known cytokine involved in intestinal inflammation during NEC, was significantly decreased in the small intestine of pups with NEC that received enteral I3C supplementation compared with their littermates treated with vehicle ($p = 0.0015$) further demonstrated by protein quantitation of IL-1β (Fig. 1F). No significant difference in the expression of the chemokine *Cxcl2* in the small intestine was observed in pups with NEC treated with I3C treatment compared with littermates treated with vehicle alone (Fig. 1G). Prior studies of AhR-deficient mice subjected to dextran sodium sulfate (DSS)–induced colitis found increased lipocalin-2 (*Lcn2*) expression in the colon compared with wild-type mice (5). In our model, we observed significantly decreased expression of *Lcn2* in pups with NEC treated with I3C compared with littermates treated with vehicle ($p = 0.0098$) (Fig. 1G). Consistent with these observations of decreased proinflammatory responses in pups supplemented with I3C during NEC, there was a significant reduction in the expression of the macrophage scavenger receptor *Marco* compared with those that received vehicle ($p = 0.0197$) (Fig. 1G). These data suggest that I3C-mediated AhR signaling reduces the expression of proinflammatory markers during NEC and implicates ligand-mediated *AhR* function as a mechanism of protection against the proinflammatory response during NEC.

RNA-seq analysis reveals a distinct gene expression profile during NEC after I3C treatment

To gain a broader understanding of the effects of I3C administration during NEC, we performed small intestinal RNA-seq analysis. We identified 126 significantly upregulated and 324 significantly downregulated genes during NEC after I3C supplementation. The comprehensive heat map and volcano plot show increased expression of *Cyp1a1* and decreased expression of *Cxcl1*, *Cxcl2*, and *Marco* (Fig. 2A, 2B). Fig. 2C identifies the most significant pathways modulated with I3C supplementation during NEC. Following our observations of improved pathology and decreased expression of *Il1b* and *Marco*, genes associated with chemokine signaling and cytokine receptor interaction pathways were also significantly downregulated with AhR ligand supplementation (Fig. 2C). We did not observe differentially expressed genes in I3C- and vehicle-treated control mice, suggesting that the effects of I3C treatment are enhanced by the NEC-mediated inflammatory setting.

Prior studies have implicated AhR activation in the production of IL-22, which has protective functions in the intestine, either by direct regulation of *Il22* gene expression or through the development of $CD4^+$ T cells and group 3 innate lymphoid cells (ILC3s) (38, 39). Further, recent work by Cho et al. (40) has shown a decrease in $RORgt^+NKp46^+$ ILC3s, which are prominent producers of IL-22, during murine NEC. Therefore, we next determined whether the protective effect of AhR activation with I3C treatment during NEC was IL-22 dependent. We observed a significant increase in the small intestine *Il22* gene expression in pups within the experimental group receiving I3C compared with vehicle control (Supplemental Fig. 2A). However, there was no significant increase in the small intestine expression of the IL-22–dependent genes *Fut2* or *Reg3g* in the NEC group treated with I3C compared with corn oil, suggesting that the protective effect of I3C treatment was independent of these genes (Supplemental Fig. 2A). Expression of *Il1b* positively correlated

with the expression of *Il22* in the small intestine during NEC (R^2 = 0.1925; p = 0.0173) (Supplemental Fig. 2B). These findings imply that these IL-22 signaling targets do not play a significant role in AhR-mediated protection observed during NEC.

With the observed increase in small intestine *Il22* in pups with NEC treated with I3C, we investigated whether I3C treatment during NEC in wild-type mice attenuates inflammation through regulatory T cell induction. A recent study by Abron et al. (41) reported that the attenuation of DSS-induced adult murine colitis by treatment with the AhR ligand ITE occurred through the induction of regulatory T cells and a reduction in $CD4^+$ T cells and inflammatory cytokines. We sought to evaluate whether treatment with I3C during experimental murine NEC could induce a similar effect. We observed no significant difference in small intestine mRNA expression of cytokines *Tnf*, *Il6*, or *Il10* during NEC in pups receiving I3C compared with vehicle treatment (Supplemental Fig. 3A). Flow cytometric analysis of isolated small intestine lamina propria cells revealed no significant induction of IL-17A, IFN-γ, or Foxp3-expressing $CD4^+$ T cells or the induction of $CD8^+$ T cells in wild-type mice with NEC or healthy controls receiving I3C treatment or the vehicle control (Supplemental Fig. 3B–E). These results suggest that treatment with AhR ligands during experimental NEC does not influence the regulatory T cell response.

Ligand-mediated AhR signaling during NEC does not influence the gut microbiota

Microbial dysbiosis, specifically an increase in Proteobacteria, has been observed in the stool of infants preceding NEC (42, 43). Therefore, changes in microbial composition can provide clues to the pathogenesis of NEC. We aimed to determine whether the administration of I3C impacted the diversity of the microbiome during experimental NEC using 16S rRNA sequencing. There was no significant difference in the overall bacterial diversity of fecal samples between the two experimental groups using the Chao1 metric for estimation of species richness or the Shannon and Simpson diversity indices (Fig. 3A, 3B). Wild-type pups subjected to NEC and treated with I3C demonstrated no statistical difference in the abundance of enteric bacterial organisms at the genus level when compared with wild-type littermates receiving the vehicle corn oil alone. (Fig. 3C). These results suggest that treatment with I3C during our short-term NEC model does not likely alter the abundance of specific microbes.

AhR signaling in intestinal epithelial cells is dispensable in experimental NEC

AhR signaling in intestinal stem cells has been shown to play a key role in regulating gut barrier homeostasis by preventing unfettered proliferation and guiding proper differentiation (44). To determine whether the observed protective effect of I3C is mediated by AhR signaling in intestinal epithelial cells (IECs), mice lacking $AhR^{\Delta IEC}$ were subjected to experimental NEC. Histology scoring of H&E-stained tissue samples from $AhR^{\Delta IEC}$ mice with NEC revealed no significant difference in the proportion of small intestine tissue sections that contained mild or severe NEC lesions when compared with cre-negative littermates (Fig. 4A, 4B). To confirm that *Ahr* was deleted in epithelial cells, the small intestine of healthy dam-fed $AhR^{\Delta IEC}$ and cre-negative mice were harvested for the isolation of the small intestine epithelial cells. Positive staining with anti-EpCAM (anti-CD326) and an absence of anti-CD45 staining confirmed positive isolation of epithelial cells and

exclusion of leukocytes, respectively (Fig. 4C). Flow cytometric analysis demonstrated significantly reduced AhR expression in $CD326^{+}CD45^{-}$ epithelial cells isolated from $AhR^{\Delta IEC}$ pups compared with cre-negative littermates (Fig. 4D). Quantitative PCR revealed a significantly reduced *Ahr* mRNA expression in isolated epithelial cells, further demonstrating *Ahr* deletion in IECs (Fig. 4E).

$AhR^{\Delta IEC}$ pups exhibited a similar inflammatory response during experimental NEC compared with their wild-type littermates, as assessed by mRNA expression of proinflammatory *Il1b* and *Cxcl2* between the two experimental NEC groups (Fig. 4F). These data suggest that $AhR^{\Delta IEC}$ mice and cre-negative littermates have a similar susceptibility to NEC and that AhR signaling in the IECs may not be significantly involved in the inflammatory response during experimental NEC.

$CD11c^{+}$ cell–specific AhR signaling is not induced during homeostasis

AhR expression in dendritic cells (DCs) is an important component in the regulation of the balance between tolerance and immunity (5, 45). AhR signaling promotes monocyte differentiation into DCs and induces tolerogenic immune responses (5, 45). The absence of AhR in $CD11c^{+}$ cells leads to exaggerated responses to LPS (46) and is associated with a dysfunctional intestinal epithelial barrier and a more severe DSS-induced colitis (5). To determine whether the protection of AhR activation during NEC is mediated by $CD11c^{+}$ cells, we evaluated AhR signaling in $CD11c^{+}$ immune cells during homeostasis. Histologic analysis revealed no significant difference in small intestine epithelial architecture under steady-state conditions in dam-fed $AhR^{\Delta CD11c}$ pups compared with their cre-negative littermates (Fig. 5A). To confirm deletion of *Ahr* in $CD11c^{+}$ cells, small intestine lamina propria cells were isolated from dam-fed $AhR^{\Delta CD11c}$ mice and cre-negative littermates. Quantitative PCR analysis revealed negligible *Ahr* mRNA expression in the enriched $CD11c^{+}$ cells from the lamina propria of $AhR^{\Delta CD11c}$ mice compared with cre-negative littermates, demonstrating *Ahr* deficiency of $CD11c^{+}$ cells (Fig. 5B). Quantitative PCR was used to evaluate the mRNA levels of IEC markers in the small intestine terminal ileum, including *olfactomedin 4* (*Olfm4*) for intestinal stem cells, *Mucin 2* (*Muc2*) for goblet cells, or *lysozyme* for Paneth cells, with no differences found between the $AhR^{\Delta CD11c}$ mice and their cre-negative littermates (Fig. 5C). As AhR signaling has been implicated in the differentiation of monocytes into DCs, we examined these cell populations by flow cytometry. There was no significant change in the percentage of $CD103^{+}CD11b^{+}$ and $CD103^{+}CD11b^{-}$ cells between $AhR^{\Delta CD11c}$ pups and cre-negative littermates at homeostasis (Fig. 5D, 5E). We then analyzed the expression of monocyte-derived intestinal tissue-resident Tim-4^{-} macrophage subsets by flow cytometry. Although we observed no difference in $CD11b^{+}CD64^{+}$ macrophages in dam-fed $AhR^{\Delta CD11c}$ and cre-negative pups at steady state, we found an increase in the Tim-4^{-} monocyte–dependent subset of macrophages in the small intestine lamina propria in $AhR^{\Delta CD11c}$ mice (Fig. 5F, 5H).

AhR activity in $CD11c^{+}$ cells mediates the severity of the inflammatory response during NEC

We next evaluated the impact of cell-intrinsic AhR signaling in $CD11c^{+}$ cells during NEC. $AhR^{\Delta CD11c}$ mice were susceptible to intestinal injury during experimental NEC, as

demonstrated by a loss of structural architecture of the intestinal villi, with significant differences in the presence of severe lesions compared with their cre-negative littermates (Fig. 6A, 6B). Although there was also no significant difference in *Cxcl2* expression between the two experimental groups, we observed that $AhR^{\Delta CD11c}$ pups with NEC experienced significantly higher small intestine mRNA expression of proinflammatory *Il1b* ($p = 0.0006$), which was confirmed by IL-1β protein quantification, suggesting increased intestinal inflammation in the $AhR^{\Delta CD11c}$ pups compared with their cre-negative littermates subjected to NEC (Fig. 6C). Flow cytometric analysis of the lamina propria DCs demonstrated no significant difference in the abundance of $CD103^+$ $CD11b^-$ or $CD103^+CD11b^+$ DC populations in cre-negative or $AhR^{\Delta CD11c}$ pups during NEC (Fig. 6D).

To further investigate the impact of AhR proligand I3C during NEC, we next evaluated the inflammatory response in $AhR^{\Delta CD11c}$ pups and cre-negative littermates treated with I3C or vehicle control during homeostasis and experimental NEC. $AhR^{\Delta CD11c}$ pups and cre-negative littermates exhibited increased proinflammatory expression of *Il1b* during NEC when compared with dam-fed controls (Supplemental Fig. 4A). Although I3C treatment during NEC in cre-negative pups attenuated inflammation when compared with those treated with the vehicle alone, this same protection was not observed in $AhR^{\Delta CD11c}$ pups. Additionally, treatment with I3C in both dam-fed mice and those subjected to NEC resulted in a significant increase in mRNA expression of *Cyp1a1* in the small intestine, although this response appeared to be dampened in $AhR^{\Delta CD11c}$ pups (Supplemental Fig. 4B). To investigate the role of the intestinal DC population in the production of proinflammatory *Il1b* in this model, the small intestine of dam-fed and experimental NEC $AhR^{\Delta CD11c}$ pups and cre-negative littermates were harvested for isolation of the lamina propria cells at the conclusion of the NEC model. Although we observed reduced survival of myeloid cells after isolation, flow cytometric analysis of the enriched $CD11c^+$ cells from the lamina propria suggested no significant difference in IL-1β in $CD11c^+CD11b^+$ or $CD11c^+CD11b^-$ DC populations in $AhR^{\Delta CD11c}$ or cre-negative controls during homeostasis or during experimental NEC (Supplemental Fig. 4C–E).

Therefore, to determine the specific immune cell type implicated in the increased relative expression of IL-1β during NEC in $AhR^{\Delta CD11c}$ pups, we then evaluated the abundance of monocyte-derived intestinal tissue-resident $Tim\text{-}4^-$ macrophages by flow cytometry from $AhR^{\Delta CD11c}$ and cre-negative pups. Importantly, we observed an increase in the $Tim\text{-}4^-$ monocyte–dependent subset of macrophages in the small intestine lamina propria in $AhR^{\Delta CD11c}$ pups during NEC compared with their cre-negative littermates (Fig. 6E, 6F). These data suggest that small intestine IL-1β production during NEC in AhR $CD11c^+$-immune cell knockouts may be mediated by the $Tim\text{-}4^-$ intestinal macrophage subset.

DISCUSSION

The identification of the intestinal inflammatory and immune cell signaling pathways involved in NEC pathogenesis is critical to the development of new therapeutics. In this study, we demonstrate that ligand-mediated AhR signaling attenuates inflammation and reduces disruption of the intestinal epithelial architecture during NEC. We also identify that AhR signaling in $CD11c^+$ immune cells may modify the inflammatory response during NEC

and now provide evidence that AhR dysregulation in IECs does not likely have a significant physiological role during NEC. We observe that AhR agonistic activity in $CD11c^+$ immune cells reduces the severity of NEC-induced inflammation, which has implications for a novel therapy targeting this specific cell type to attenuate the inflammatory response during NEC.

The roles of endogenous and exogenous AhR ligands in intestinal homeostasis and the inflammatory response have been previously described. Disruption in AhR signaling is implicated in animal models of gastrointestinal diseases, such as intestinal malignancies and adult colitis (5, 47). AhR activation by dietary ligands in a model of azoxymethane/DSS-induced tumorigenesis resulted in a reduction of tumor burden and impaired epithelial repair through regulation of differentiation and protection from inflammation-induced tumorigenesis (10). Tryptophan metabolites derived from the gut microbiome may also function as AhR ligands (15, 48, 49). Bacteria-derived indole metabolites as AhR agonists have been implicated in the maintenance of the integrity of the mucosal and epithelial barrier (7, 49). In addition, exogenous AhR agonists can affect intestinal homeostasis and impact gastrointestinal diseases. Mokshagundam et al. (50) demonstrated that in utero exposure to the environmental toxin 2,3,7,8-tetrachlorodibenzo-*p*-dioxin, a potent AhR agonist, promoted the development of NEC. In contrast, exogenous dietary AhR proligands, such as I3C, influence the postnatal expansion of intestinal innate lymphoid cells to protect against intestinal infections (11, 39, 51). Recent findings have shown that loss of AhR induces carcinogenesis and cecal tumor incidence, whereas dietary administration of agonistic AhR proligands such as I3C or diindolylmethane can serve as critical regulators of intestinal mucosal homeostasis (47, 52). Other signaling pathways involved in maintaining intestinal homeostasis include the IL-22 signaling pathway. AhR activity is known to be essential for IL-22 production in the intestinal lamina propria and protection against intestinal bacterial infection (39, 53). However, in our study, with no significant difference in *Fut2* or *Reg3g* expression in the experimental groups, we observed that AhR proligand supplementation during NEC occurs independently of IL-22.

As an increase in *Il22* mRNA expression in the small intestine was seen in pups with NEC treated with I3C, we aimed to investigate if treatment with I3C during NEC attenuates inflammation via the regulatory T cell response. In a model of adult murine DSS-colitis by Abron et al. (41) treatment with AhR ligand ITE induced regulatory T cells and reduced $CD4^+$ T cells and inflammatory cytokines. Further, prior research by Egan et al. (54) has suggested a predominance of $CD4^+$ T lymphocytes in experimental NEC and, in particular, $CD4^+$ T_H17 cells. However, in our studies with younger mice, treatment with the AhR proligand I3C during NEC did not result in a significant increase in small intestine mRNA expression of cytokines *Tnf*, *Il6*, or *Il10* during NEC or the significant induction of IL-17A, IFN-γ, or Foxp3-expressing $CD4^+$ T cells or the induction of $CD8^+$ T cells compared with wild-type pups with NEC treated with I3C or the vehicle control. This observed limited T cell response may be attributed to the limited expansion and differentiation of T cells, including regulatory T cells, in neonatal mice (55, 56). Notably, immaturity of the T cell compartment is also observed in extremely preterm human infants, increasing their susceptibility to infection and impairing their immune functions, which may predispose them to NEC development (57).

The current study describes the role of the enteral AhR proligand I3C in attenuating the inflammatory response during NEC. Specifically, we demonstrate that I3C supplementation reduces NEC severity and downregulates the expression of proinflammatory *Il1b* and *Lcn2* during NEC. Recent findings have shown the anti-inflammatory role of AhR in the inhibition of NLRP3 inflammasome formation and caspase-1 activity and, therefore, subsequent IL-1β production, as the derivation of IL-1β from its precursor is mediated by caspase-1 (58, 59). To further investigate the transcriptional profile after I3C treatment on the gut inflammatory response during NEC, we performed RNA-seq. Transcriptional analysis revealed a distinct gene expression profile in the small intestine (≥2-fold, $p < 0.05$) following I3C treatment when compared with vehicle control during experimental NEC. The expression of genes involved in cytokine–cytokine receptor interaction and chemokine signaling; specifically, *Ccl9*, *Gng4*, *Osmr*, *Inhba*, *Tnfrsf25*, *Tnfrsf13b*, *Rasgrp2*, *Xcr1*, and *Csf3r* were decreased in pups with NEC treated with I3C.

We also show that the effect of exogenous I3C administration was not associated with changes in fecal microbial diversity. Prior investigations have provided evidence for the ability of the dietary metabolites to activate the AhR signaling pathway and influence the composition of the microbiome in the small intestine (60). In our model, the microbiota did not play a significant role during AhR-mediated attenuation of NEC-induced inflammation. This may be attributed to the enteric delivery of a human microbiome in the animals' formula to induce NEC in neonatal mice.

Prior studies have shown impairment of colonic crypt stem cells in IEC-specific AhR knockouts in mouse models. Specifically, adult $AhR^{\Delta IEC}$ mice are more sensitive to DSS-induced colitis and intestinal inflammation when compared with controls, suggesting a role of AhR in IEC integrity (10, 61). Additionally, the deletion of AhR in IECs is known to disrupt the integrity of the intestinal barrier and impairs epithelial cell differentiation from intestinal crypt stem cells (10, 62). In particular, Metidji et al. (10) have demonstrated that IEC-specific deletion of AhR during *Citrobacter rodentium* infection resulted in lower expression of *Muc2* and higher expression of proinflammatory *Il6* and that AhR activation by the dietary AhR proligand I3C restored the negative feedback control of Wnt/β-catenin signaling, a pathway that has been previously implicated in NEC intestinal injury (63). Findings from Alvarado et al. (14) revealed that upregulation of IDO1, an enzyme in tryptophan metabolism for endogenous AhR ligand derivation, resulted in increased secretory cell differentiation, increased mucous production in the epithelium, and reduced epithelial damage. Recent findings from Lu et al. (64) demonstrated increased NEC severity in AhR IEC–specific knockout mice as described by a higher expression of proinflammatory *Il6* and *Tnf-α* and more severe histology scores. However, in our studies using younger neonatal mice, we observe $AhR^{\Delta IEC}$ pups to display a similar susceptibility to NEC compared with cre-negative littermates with no significant difference in expression of proinflammatory cytokines or chemokines and no significant difference in intestinal morphology of the terminal ileum. Therefore, we conclude that in our mouse model of NEC, AhR signaling in IECs is unlikely to be responsible for the exaggerated inflammatory response seen.

AhR activation has a role in the differentiation of monocytes to macrophages or DCs, a necessary action during an inflammatory response (45). These cells within the lamina propria have a necessary role in sampling Ags within the intestinal luminal space through interepithelial dendritic extension (5). A prior investigation has demonstrated that the interaction of LPS with AhR-deficient peritoneal macrophages induces proinflammatory cytokine production, including IL-6 and TNF-α (65). Additionally, similar to AhR deficiency, signal transducer and activator of transcription 1 (Stat1) deficiency resulted in an LPS-induced IL-4 production, indicating an essential role of AhR in the negative regulation of the LPS signaling pathway through interaction with Stat1 (65).

Similarly, our current findings demonstrate increased small intestine proinflammatory *Il1b* expression in $AhR^{\Delta CD11c}$ pups with NEC. In this model, we did not observe a significant difference in the *Cxcl2* chemokine response during the NEC-induced inflammatory response between the two experimental groups. As it is unlikely that increased small intestine proinflammatory *Il1b* during NEC in $AhR^{\Delta CD11c}$ pups is attributed to AhR activity in intestinal DCs, we now provide evidence that activation of AhR in $CD11c^{+}$ immune cells may be specific to Tim-4 resident intestinal macrophages of the lamina propria. Resident intestinal macrophages are a monocyte-derived population with distinct subsets. In particular, the $Tim\text{-}4^{-}$ macrophage subset has a high turnover from monocytes and is dependent on CCR2-mediated monocyte recruitment (66, 67). In contrast, $Tim4^{+}$ macrophages are highly represented perinatally and in the neonatal small intestine (66). These data suggest that the inflammatory response during NEC in $CD11c^{+}$ immune cell knockouts may be driven by the $Tim\text{-}4^{-}$ intestinal macrophage subset.

We conclude that AhR agonistic activity mediated by the exogenous dietary AhR proligand I3C mitigates the proinflammatory response during NEC. Further, we suggest that the mechanism mediating this protective effect of I3C occurs in an immune cell–specific manner and, more specifically, may be mediated by resident intestinal macrophages. Additional investigation is required to investigate the role of resident intestinal macrophages in NEC pathophysiology. Taken together, we have now identified an additional signaling pathway involved in the pathogenesis of NEC and provide the possibility for a new therapeutic approach for this fatal disease.

Supplementary Material

Refer to Web version on PubMed Central for supplementary material.

ACKNOWLEDGMENTS

We thank Dr. Jay Kolls at Tulane School of Medicine for feedback on these studies and review of the manuscript. We also thank the Bursky Center for Human Immunology and Immunotherapy Programs at Washington University, Immunomonitoring Laboratory.

This work was supported by the National Institutes of Health (NIH) R01DK118568 (to M.G.), R03DK111473 (to M.G.), K08DK101608 (to M.G.), and 5T32HD043010 (to L.S.N.); March of Dimes Foundation Grant 5-FY17-79 (to M.G.); the American Academy of Pediatrics Marshall Klaus Award (to L.S.N.), the St. Louis Children's Hospital Foundation (to M.G.); the Children's Discovery Institute (CDI) of Washington University School of Medicine (WUSM); and the St. Louis Children's Hospital (SLCH) and the Department of Pediatrics at WUSM. Contributions from the Genome Technology Access Center in the Department of Genetics at WUSM are partially supported by National Cancer Institute Cancer Center Support Grant P30 CA91842 to the Siteman Cancer Center,

by the Institute for Clinical and Translational Science Clinical and Translational Sciences Award, National Center for Research Resources of the NIH Grant UL1TR000448, and the NIH Roadmap for Medical Research. Contributions from the WUSM Digestive Disease Research Core Center are supported by NIH Grant P30DK052574. Imaging contributions were performed in part through the use of the Washington University Center for Cellular Imaging supported by WUSM, the CDI of WUSM and SLCH (CDI-CORE-2015-505 and CDI-CORE-2019-813), and the Foundation for Barnes-Jewish Hospital (3770 and 4642). None of the funding sources had any role in the manuscript.

DISCLOSURES

M.G. has received sponsored research agreement funding from Astarte Medical Partners, Takeda Pharmaceuticals, and Evive Biotech, Inc. She also participated in a neonatal microbiome advisory board for Abbott Laboratories. None of these sources had any role in this study. The other authors have no financial conflicts of interest.

Abbreviations used in this article:

AhR	aryl hydrocarbon receptor
AhR$^{\Delta CD11c}$	AhR in dendritic cell
AhR$^{\Delta IEC}$	AhR expression in intestinal epithelial cell
DC	dendritic cell
DSS	dextran sodium sulfate
I3C	indole-3-carbinol
IEC	intestinal epithelial cell
KEGG	Kyoto Encyclopedia of Genes and Genomes
Lcn2	lipocalin-2
Muc2	*Mucin 2*
NEC	necrotizing enterocolitis
Olfm4	*olfactomedin 4*
P	postnatal day-of-life
qRT-PCR	quantitative real-time PCR
RNA-seq	RNA sequencing

REFERENCES

1. Maloy KJ, and Powrie F. 2011. Intestinal homeostasis and its breakdown in inflammatory bowel disease. Nature 474: 298–306. [PubMed: 21677746]
2. Neu J, and Walker WA. 2011. Necrotizing enterocolitis. N. Engl. J. Med 364: 255–264. [PubMed: 21247316]
3. Lin PW, and Stoll BJ. 2006. Necrotising enterocolitis. Lancet 368: 1271–1283. [PubMed: 17027734]
4. De Plaen IG 2013. Inflammatory signaling in necrotizing enterocolitis. Clin. Perinatol 40: 109–124. [PubMed: 23415267]

5. Chng SH, Kundu P, Dominguez-Brauer C, Teo WL, Kawajiri K, Fujii-Kuriyama Y, Mak TW, and Pettersson S. 2016. Ablating the aryl hydrocarbon receptor (AhR) in CD11c+ cells perturbs intestinal epithelium development and intestinal immunity. Sci. Rep 6: 23820. [PubMed: 27068235]
6. Takamura T, Harama D, Matsuoka S, Shimokawa N, Nakamura Y, Okumura K, Ogawa H, Kitamura M, and Nakao A. 2010. Activation of the aryl hydrocarbon receptor pathway may ameliorate dextran sodium sulfate-induced colitis in mice. Immunol. Cell Biol 88: 685–689. [PubMed: 20231854]
7. Qiu J, Heller JJ, Guo X, Chen ZM, Fish K, Fu Y-X, and Zhou L. 2012. The aryl hydrocarbon receptor regulates gut immunity through modulation of innate lymphoid cells. Immunity 36: 92–104. [PubMed: 22177117]
8. Esser C, and Rannug A. 2015. The aryl hydrocarbon receptor in barrier organ physiology, immunology, and toxicology. Pharmacol. Rev 67: 259–279. [PubMed: 25657351]
9. Shi LZ, Faith NG, Nakayama Y, Suresh M, Steinberg H, and Czuprynski CJ. 2007. The aryl hydrocarbon receptor is required for optimal resistance to *Listeria monocytogenes* infection in mice. J. Immunol 179: 6952–6962. [PubMed: 17982086]
10. Metidji A, Omenetti S, Crotta S, Li Y, Nye E, Ross E, Li V, Maradana MR, Schiering C, and Stockinger B. 2018. The environmental sensor AHR protects from inflammatory damage by maintaining intestinal stem cell homeostasis and barrier integrity. [Published erratum appears in 2019 Immunity 50: 1542.] Immunity 49: 353–362.e5. [PubMed: 30119997]
11. Kiss EA, Vonarbourg C, Kopfmann S, Hobeika E, Finke D, Esser C, and Diefenbach A. 2011. Natural aryl hydrocarbon receptor ligands control organogenesis of intestinal lymphoid follicles. Science 334: 1561–1565. [PubMed: 22033518]
12. Brawner KM, Yeramilli VA, Duck LW, Van Der Pol W, Smythies LE, Morrow CD, Elson CO, and Martin CA. 2019. Depletion of dietary aryl hydrocarbon receptor ligands alters microbiota composition and function. Sci. Rep 9: 14724. [PubMed: 31604984]
13. Aoki R, Aoki-Yoshida A, Suzuki C, and Takayama Y. 2018. Indole-3-pyruvic acid, an aryl hydrocarbon receptor activator, suppresses experimental colitis in mice. J. Immunol 201: 3683–3693. [PubMed: 30429284]
14. Alvarado DM, Chen B, Iticovici M, Thaker AI, Dai N, VanDussen KL, Shaikh N, Lim CK, Guillemin GJ, Tarr PI, and Ciorba MA. 2019. Epithelial indoleamine 2,3-dioxygenase 1 modulates aryl hydrocarbon receptor and notch signaling to increase differentiation of secretory cells and alter mucus-associated microbiota. Gastroenterology 157: 1093–1108.e11. [PubMed: 31325428]
15. Jin U-H, Lee S-O, Sridharan G, Lee K, Davidson LA, Jayaraman A, Chapkin RS, Alaniz R, and Safe S. 2014. Microbiome-derived tryptophan metabolites and their aryl hydrocarbon receptor-dependent agonist and antagonist activities. Mol. Pharmacol 85: 777–788. [PubMed: 24563545]
16. DiNatale BC, Murray IA, Schroeder JC, Flaveny CA, Lahoti TS, Laurenzana EM, Omiecinski CJ, and Perdew GH. 2010. Kynurenic acid is a potent endogenous aryl hydrocarbon receptor ligand that synergistically induces interleukin-6 in the presence of inflammatory signaling. Toxicol. Sci 115: 89–97. [PubMed: 20106948]
17. Nebert DW, Dalton TP, Okey AB, and Gonzalez FJ. 2004. Role of aryl hydrocarbon receptor-mediated induction of the CYP1 enzymes in environmental toxicity and cancer. J. Biol. Chem 279: 23847–23850. [PubMed: 15028720]
18. Li Y, Innocentin S, Withers DR, Roberts NA, Gallagher AR, Grigorieva EF, Wilhelm C, and Veldhoen M. 2011. Exogenous stimuli maintain intraepithelial lymphocytes via aryl hydrocarbon receptor activation. Cell 147: 629–640. [PubMed: 21999944]
19. Anderton MJ, Manson MM, Verschoyle RD, Gescher A, Lamb JH, Farmer PB, Steward WP, and Williams ML. 2004. Phar-macokinetics and tissue disposition of indole-3-carbinol and its acid condensation products after oral administration to mice. Clin. Cancer Res 10: 5233–5241. [PubMed: 15297427]
20. Martin B, Hirota K, Cua DJ, Stockinger B, and Veldhoen M. 2009. Interleukin-17-producing gammadelta T cells selectively expand in response to pathogen products and environmental signals. Immunity 31: 321–330. [PubMed: 19682928]

21. Gopalakrishna KP, Macadangdang BR, Rogers MB, Tometich JT, Firek BA, Baker R, Ji J, Burr AHP, Ma C, Good M, et al. 2019. Maternal IgA protects against the development of necrotizing enterocolitis in preterm infants. Nat. Med 25: 1110–1115. [PubMed: 31209335]
22. Good M, Sodhi CP, Egan CE, Afrazi A, Jia H, Yamaguchi Y, Lu P, Branca MF, Ma C, Prindle T Jr., et al. 2015. Breast milk protects against the development of necrotizing enterocolitis through inhibition of Toll-like receptor 4 in the intestinal epithelium via activation of the epidermal growth factor receptor. Mucosal Immunol 8: 1166–1179. [PubMed: 25899687]
23. Good M, Sodhi CP, Yamaguchi Y, Jia H, Lu P, Fulton WB, Martin LY, Prindle T, Nino DF, Zhou Q, et al. 2016. The human milk oligosaccharide 2'-fucosyllactose attenuates the severity of experimental necrotising enterocolitis by enhancing mesenteric perfusion in the neonatal intestine. Br. J. Nutr 116: 1175–1187. [PubMed: 27609061]
24. Good M, Sodhi CP, Ozolek JA, Buck RH, Goehring KC, Thomas DL, Vikram A, Bibby K, Morowitz MJ, Firek B, et al. 2014. *Lactobacillus* rhamnosus HN001 decreases the severity of necrotizing enterocolitis in neonatal mice and preterm piglets: evidence in mice for a role of TLR9. Am. J. Physiol. Gastrointest. Liver Physiol 306: G1021–G1032. [PubMed: 24742987]
25. Shertzer HG, and Sainsbury M. 1991. Intrinsic acute toxicity and hepatic enzyme inducing properties of the chemoprotectants indole-3-carbinol and 5,10-dihydroindeno[1,2-b]indole in mice. Food Chem. Toxicol 29: 237–242. [PubMed: 2040485]
26. National Toxicology Program. 2017. NTP technical report on the toxicology studies of indole-3-carbinol (CASRN 700-06-1) in F344/N rats and B6C3F1/N mice and toxicology and carcinogenesis studies of indole-3-carbinol in harlan sprague dawley rats and B6C3F1/N mice (gavage studies). NTP Tech. Rep 584: 1–87.
27. Dobin A, Davis CA, Schlesinger F, Drenkow J, Zaleski C, Jha S, Batut P, Chaisson M, and Gingeras TR. 2013. STAR: ultrafast universal RNA-seq aligner. Bioinformatics 29: 15–21. [PubMed: 23104886]
28. Liao Y, Smyth GK, and Shi W. 2014. featureCounts: an efficient general purpose program for assigning sequence reads to genomic features. Bioinformatics 30: 923–930. [PubMed: 24227677]
29. Patro R, Duggal G, Love MI, Irizarry RA, and Kingsford C. 2017. Salmon provides fast and bias-aware quantification of transcript expression. Nat. Methods 14: 417–419. [PubMed: 28263959]
30. Wang L, Wang S, and Li W. 2012. RSeQC: quality control of RNA-seq experiments. Bioinformatics 28: 2184–2185. [PubMed: 22743226]
31. Robinson MD, McCarthy DJ, and Smyth GK. 2010. edgeR: a Bioconductor package for differential expression analysis of digital gene expression data. Bioinformatics 26: 139–140. [PubMed: 19910308]
32. Ritchie ME, Phipson B, Wu D, Hu Y, Law CW, Shi W, and Smyth GK. 2015. Limma powers differential expression analyses for RNA-sequencing and microarray studies. Nucleic Acids Res 43: e47. [PubMed: 25605792]
33. Liu R, Holik AZ, Su S, Jansz N, Chen K, Leong HS, Blewitt ME, Asselin-Labat M-L, Smyth GK, and Ritchie ME. 2015. Why weight? Modelling sample and observational level variability improves power in RNA-seq analyses. Nucleic Acids Res 43: e97. [PubMed: 25925576]
34. Luo W, Friedman MS, Shedden K, Hankenson KD, and Woolf PJ. 2009. GAGE: generally applicable gene set enrichment for pathway analysis. BMC Bioinformatics 10: 161. [PubMed: 19473525]
35. Luo W, and Brouwer C. 2013. Pathview: an R/Bioconductor package for pathway-based data integration and visualization. Bioinformatics 29: 1830–1831. [PubMed: 23740750]
36. Gracz AD, Puthoff BJ, and Magness ST. 2012. Identification, isolation, and culture of intestinal epithelial stem cells from murine intestine. Methods Mol. Biol 879: 89–107. [PubMed: 22610555]
37. Meng D, Sommella E, Salviati E, Campiglia P, Ganguli K, Djebali K, Zhu W, and Walker WA. 2020. Indole-3-lactic acid, a metabolite of tryptophan, secreted by Bifidobacterium longum subspecies infantis is anti-inflammatory in the immature intestine. Pediatr. Res 88: 209–217. [PubMed: 31945773]
38. Wagage S, Harms Pritchard G, Dawson L, Buza EL, Sonnenberg GF, and Hunter CA. 2015. The group 3 innate lymphoid cell defect in aryl hydrocarbon receptor deficient mice is associated with T cell hyperactivation during intestinal infection. PLoS One 10: e0128335. [PubMed: 26010337]

39. Lee JS, Cella M, McDonald KG, Garlanda C, Kennedy GD, Nukaya M, Mantovani A, Kopan R, Bradfield CA, Newberry RD, and Colonna M. 2011. AHR drives the development of gut ILC22 cells and postnatal lymphoid tissues via pathways dependent on and independent of Notch. Nat. Immunol 13: 144–151. [PubMed: 22101730]
40. Cho SX, Rudloff I, Lao JC, Pang MA, Goldberg R, Bui CB, McLean CA, Stock M, Klassert TE, Slevogt H, et al. 2020. Characterization of the pathoimmunology of necrotizing enterocolitis reveals novel therapeutic opportunities. Nat. Commun 11: 5794. [PubMed: 33188181]
41. Abron JD, Singh NP, Mishra MK, Price RL, Nagarkatti M, Nagarkatti PS, and Singh UP. 2018. An endogenous aryl hydrocarbon receptor ligand, ITE, induces regulatory T cells and ameliorates experimental colitis. Am. J. Physiol. Gastrointest. Liver Physiol 315: G220–G230. [PubMed: 29672155]
42. Torrazza RM, Ukhanova M, Wang X, Sharma R, Hudak ML, Neu J, and Mai V. 2013. Intestinal microbial ecology and environmental factors affecting necrotizing enterocolitis. PLoS One 8: e83304. [PubMed: 24386174]
43. Patel RM, and Denning PW. 2015. Intestinal microbiota and its relationship with necrotizing enterocolitis. Pediatr. Res 78: 232–238. [PubMed: 25992911]
44. Cervantes-Barragan L, and Colonna M. 2018. AHR signaling in the development and function of intestinal immune cells and beyond. Semin. Immunopathol 40: 371–377. [PubMed: 29951906]
45. Goudot C, Coillard A, Villani A-C, Gueguen P, Cros A, Sarkizova S, Tang-Huau T-L, Bohec M, Baulande S, Hacohen N, et al. 2017. Aryl hydrocarbon receptor controls monocyte differentiation into dendritic cells versus macrophages. Immunity 47: 582–596.e6. [PubMed: 28930664]
46. Cella M, and Colonna M. 2015. Aryl hydrocarbon receptor: Linking environment to immunity. Semin. Immunol 27: 310–314. [PubMed: 26561251]
47. Ikuta T, Kobayashi Y, Kitazawa M, Shiizaki K, Itano N, Noda T, Pettersson S, Poellinger L, Fujii-Kuriyama Y, Taniguchi S, and Kawajiri K. 2013. ASC-associated inflammation promotes cecal tumorigenesis in aryl hydrocarbon receptor-deficient mice. Carcinogenesis 34: 1620–1627. [PubMed: 23455376]
48. Natividad JM, Agus A, Planchais J, Lamas B, Jarry AC, Martin R, Michel M-L, Chong-Nguyen C, Roussel R, Straube M, et al. 2018. Impaired aryl hydrocarbon receptor ligand production by the gut microbiota is a key factor in metabolic syndrome. Cell Metab 28: 737–749.e4. [PubMed: 30057068]
49. Zelante T, Iannitti RG, Cunha C, De Luca A, Giovannini G, Pieraccini G, Zecchi R, D'Angelo C, Massi-Benedetti C, Fallarino F, et al. 2013. Tryptophan catabolites from microbiota engage aryl hydrocarbon receptor and balance mucosal reactivity via interleukin-22. Immunity 39: 372–385. [PubMed: 23973224]
50. Mokshagundam S, Ding T, Rumph JT, Dallas M, Stephens VR, Osteen KG, and Bruner-Tran KL. 2020. Developmental 2,3,7,8-tetrachlorodibenzo-p-dioxin exposure of either parent enhances the risk of necrotizing enterocolitis in neonatal mice. Birth Defects Res 112: 1209–1223. [PubMed: 32519502]
51. Liu X, Hu H, Fan H, Zuo D, Shou Z, Liao Y, Nan Z, and Tang Q. 2017. The role of STAT3 and AhR in the differentiation of CD4+ T cells into Th17 and Treg cells. Medicine (Baltimore) 96: e6615. [PubMed: 28445259]
52. Zhao H, Chen L, Yang T, Feng Y-L, Vaziri ND, Liu B-L, Liu Q-Q, Guo Y, and Zhao Y-Y. 2019. Aryl hydrocarbon receptor activation mediates kidney disease and renal cell carcinoma. J. Transl. Med 17: 302. [PubMed: 31488157]
53. Monteleone I, Rizzo A, Sarra M, Sica G, Sileri P, Biancone L, MacDonald TT, Pallone F, and Monteleone G. 2011. Aryl hydrocarbon receptor-induced signals up-regulate IL-22 production and inhibit inflammation in the gastrointestinal tract. Gastroenterology 141: 237–248.e1 [PubMed: 21600206]
54. Egan CE, Sodhi CP, Good M, Lin J, Jia H, Yamaguchi Y, Lu P, Ma C, Branca MF, Weyandt S, et al. 2016. Toll-like receptor 4-mediated lymphocyte influx induces neonatal necrotizing enterocolitis. J. Clin. Invest 126: 495–508. [PubMed: 26690704]
55. Debock I, and Flamand V. 2014. Unbalanced neonatal CD4(+) T-cell immunity. Front. Immunol 5: 393. [PubMed: 25221551]

56. Fontenot JD, Dooley JL, Farr AG, and Rudensky AY. 2005. Developmental regulation of Foxp3 expression during ontogeny. J. Exp. Med 202: 901–906. [PubMed: 16203863]
57. Qazi KR, Bach Jensen G, van der Heiden M, Björkander S, Holmlund U, Haileselassie Y, Kokkinou E, Marchini G, Jenmalm MC, Abrahamsson T, and Sverremark-Ekström E. 2020. Extremely preterm infants have significant alterations in their conventional T cell compartment during the first weeks of life. J. Immunol 204: 68–77. [PubMed: 31801814]
58. Huai W, Zhao R, Song H, Zhao J, Zhang L, Zhang L, Gao C, Han L, and Zhao W. 2014. Aryl hydrocarbon receptor negatively regulates NLRP3 inflammasome activity by inhibiting NLRP3 transcription. Nat. Commun 5: 4738. [PubMed: 25141024]
59. Sekine H, Mimura J, Oshima M, Okawa H, Kanno J, Igarashi K, Gonzalez FJ, Ikuta T, Kawajiri K, and Fujii-Kuriyama Y. 2009. Hypersensitivity of aryl hydrocarbon receptor-deficient mice to lipopolysaccharide-induced septic shock. Mol. Cell. Biol 29: 6391–6400. [PubMed: 19822660]
60. Korecka A, Dona A, Lahiri S, Tett AJ, Al-Asmakh M, Braniste V, D'Arienzo R, Abbaspour A, Reichardt N, Fujii-Kuriyama Y, et al. 2016. Bidirectional communication between the aryl hydrocarbon receptor (AhR) and the microbiome tunes host metabolism. NPJ Biofilms Microbiomes 2: 16014. [PubMed: 28721249]
61. Chinen I, Nakahama T, Kimura A, Nguyen NT, Takemori H, Kumagai A, Kayama H, Takeda K, Lee S, Hanieh H, et al. 2015. The aryl hydrocarbon receptor/microRNA-212/132 axis in T cells regulates IL-10 production to maintain intestinal homeostasis. Int. Immunol 27: 405–415. [PubMed: 25862525]
62. Schiering C, Wincent E, Metidji A, Iseppon A, Li Y, Potocnik AJ, Omenetti S, Henderson CJ, Wolf CR, Nebert DW, and Stockinger B. 2017. Feedback control of AHR signalling regulates intestinal immunity. Nature 542: 242–245. [PubMed: 28146477]
63. Li B, Lee C, Cadete M, Zhu H, Koike Y, Hock A, Wu RY, Botts SR, Minich A, Alganabi M, et al. 2019. Impaired Wnt/β-catenin pathway leads to dysfunction of intestinal regeneration during necrotizing enterocolitis. Cell Death Dis 10: 743. [PubMed: 31582728]
64. Lu P, Yamaguchi Y, Fulton WB, Wang S, Zhou Q, Jia H, Kovler ML, Salazar AG, Sampah M, Prindle T Jr., et al. 2021. Maternal aryl hydrocarbon receptor activation protects newborns against necrotizing enterocolitis. Nat. Commun 12: 1042. [PubMed: 33589625]
65. Kimura A, Naka T, Nakahama T, Chinen I, Masuda K, Nohara K, Fujii-Kuriyama Y, and Kishimoto T. 2009. Aryl hydrocarbon receptor in combination with Stat1 regulates LPS-induced inflammatory responses. J. Exp. Med 206: 2027–2035. [PubMed: 19703987]
66. Shaw TN, Houston SA, Wemyss K, Bridgeman HM, Barbera TA, Zangerle-Murray T, Strangward P, Ridley AJL, Wang P, Tamoutounour S, et al. 2018. Tissue-resident macrophages in the intestine are long lived and defined by Tim-4 and CD4 expression. J. Exp. Med 215: 1507–1518. [PubMed: 29789388]
67. Kobayashi N, Karisola P, Peña-Cruz V, Dorfman DM, Jinushi M, Umetsu SE, Butte MJ, Nagumo H, Chernova I, Zhu B, et al. 2007. TIM-1 and TIM-4 glycoproteins bind phosphatidylserine and mediate uptake of apoptotic cells. Immunity 27: 927–940. [PubMed: 18082433]

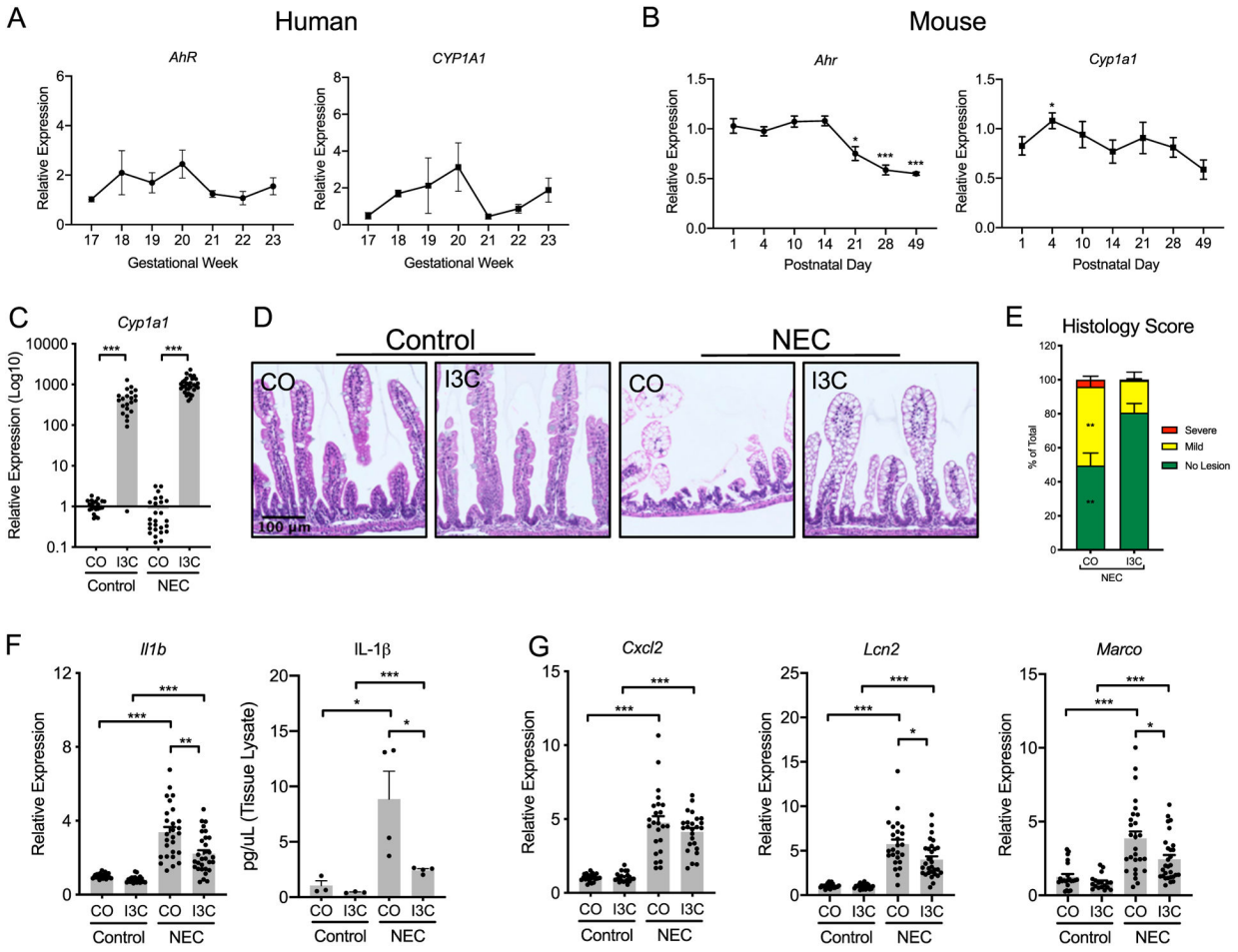

FIGURE 1. I3C-mediated AhR signaling attenuates inflammation during experimental NEC.

AhR and *CYP1A1* ontogeny are shown in (**A**) human fetal intestine for comparison with *Ahr* and *Cyp1a1* ontogeny in (**B**) P1–49 mouse pups. (**C**) Treatment with AhR proligand I3C in control and experimental NEC pups produces a significant increase in *Cyp1a1* expression, indicating activation of AhR signaling. (**D**) Representative images of formalin-fixed, paraffin-embedded murine terminal ileum tissue sections stained with H&E were used to quantify villi metrics and demonstrate I3C-mediated protection against intestinal barrier damage during NEC. (**E**) Blinded histology scoring quantitates the severity of intestinal lesions in the control and experimental groups with and without I3C treatment. (**F**) Terminal ileum expression of *Il1b* qRT-PCR (left) and protein concentration (right) is attenuated during NEC with I3C treatment. (**G**) *Cxcl2*, *Lcn2*, and *Marco* terminal ileal expression in wild-type control and I3C-fed pups with and without NEC. Data represent mean ± SEM from at least three independent experiments. *$p < 0.05$, **$p < 0.005$, ***$p < 0.0001$ by Mann–Whitney *U* test [(A)–(G) except (F), right, by unpaired *t* test]. CO, corn oil.

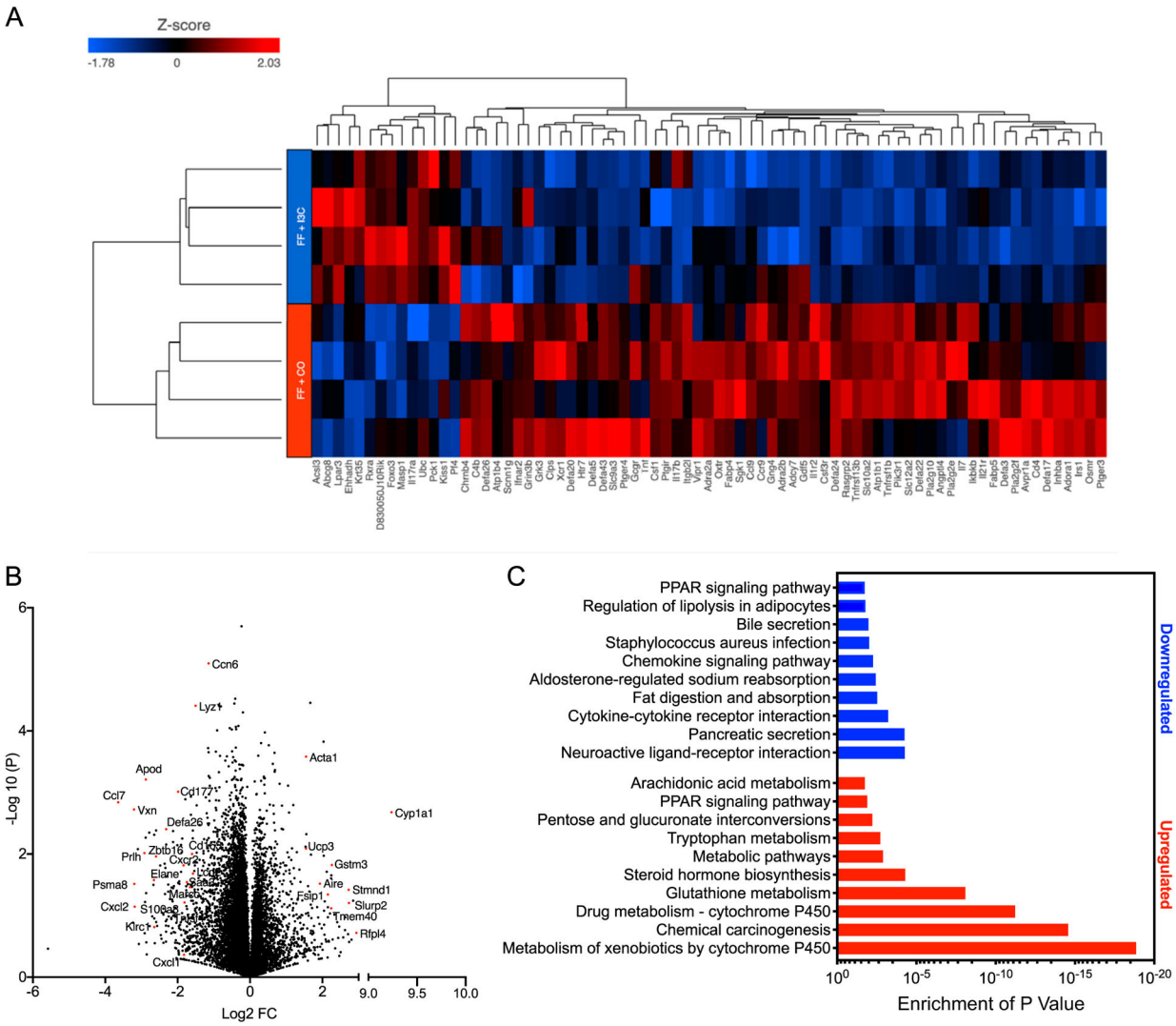

FIGURE 2. AhR activity during NEC induces a distinct profile of expressed proinflammatory response genes.

(**A**) Heat map representation of targeted genes in the experimental NEC groups with and without I3C exposure (fold change of at least 2-fold; $p \leq 0.05$). (**B**) Volcano plot provides a comparison of gene expression in experimental NEC pups with I3C supplementation and demonstrates a profile of differentially expressed genes that are upregulated and downregulated during NEC. (**C**) Functionally enriched pathways provide a comparative analysis between the experimental NEC groups. Downregulation of chemokine signaling pathways and cytokine receptor interaction pathways occurred with AhR proligand supplementation during experimental NEC. CO, corn oil.

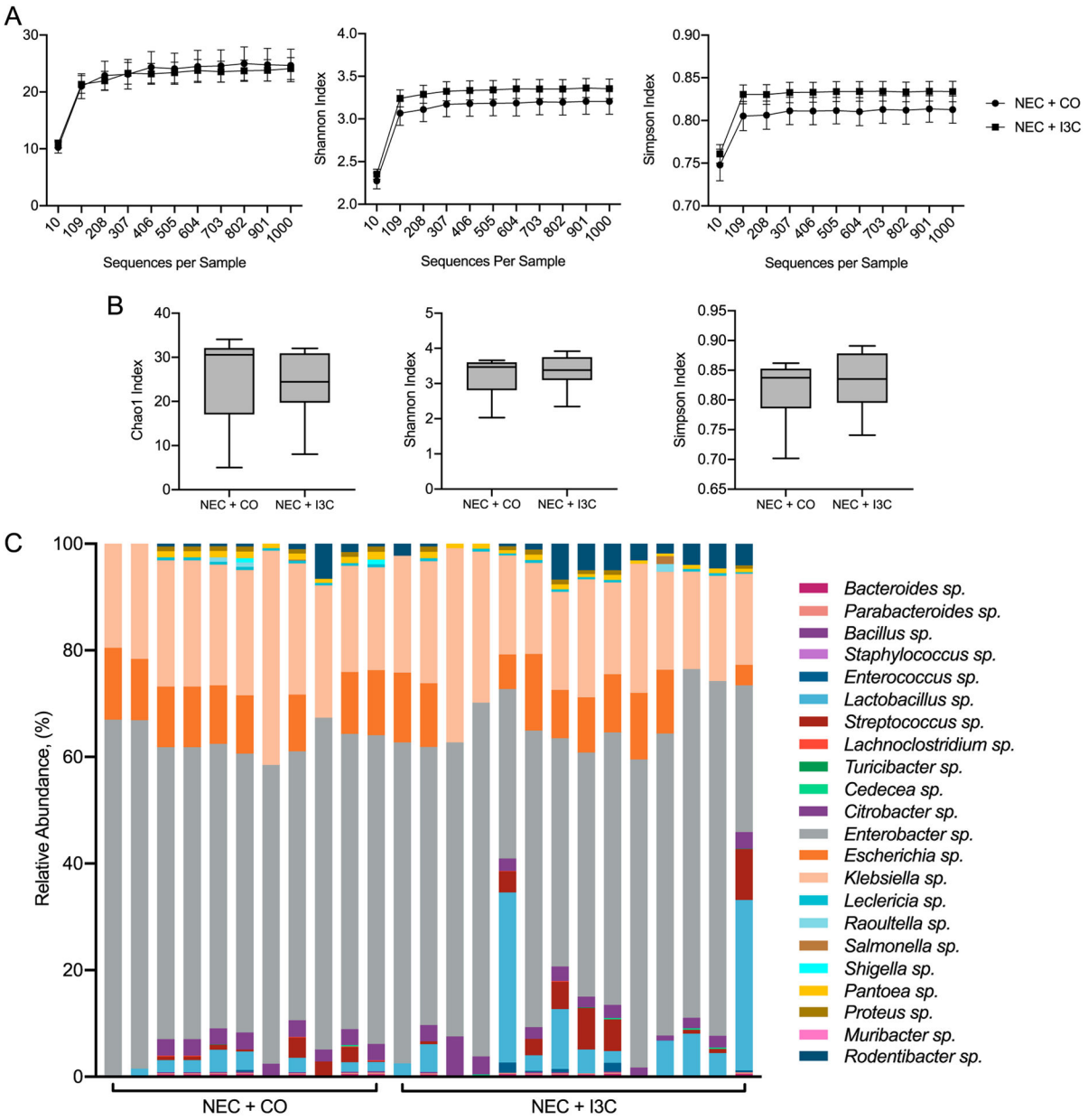

FIGURE 3. Enteral supplementation with I3C during NEC does not influence the gut microbiota.

The microbiota of fecal samples from murine NEC was evaluated using 16S ribosomal RNA-seq methods. (**A** and **B**) No significant difference in overall bacterial diversity was observed in the wild-type experimental NEC groups treated with I3C or the vehicle control, as shown by the Chao1, Shannon, and Simpson indices. (**C**) The relative abundance of selected bacteria in the experimental NEC groups is shown with no significant difference among the groups. CO, corn oil.

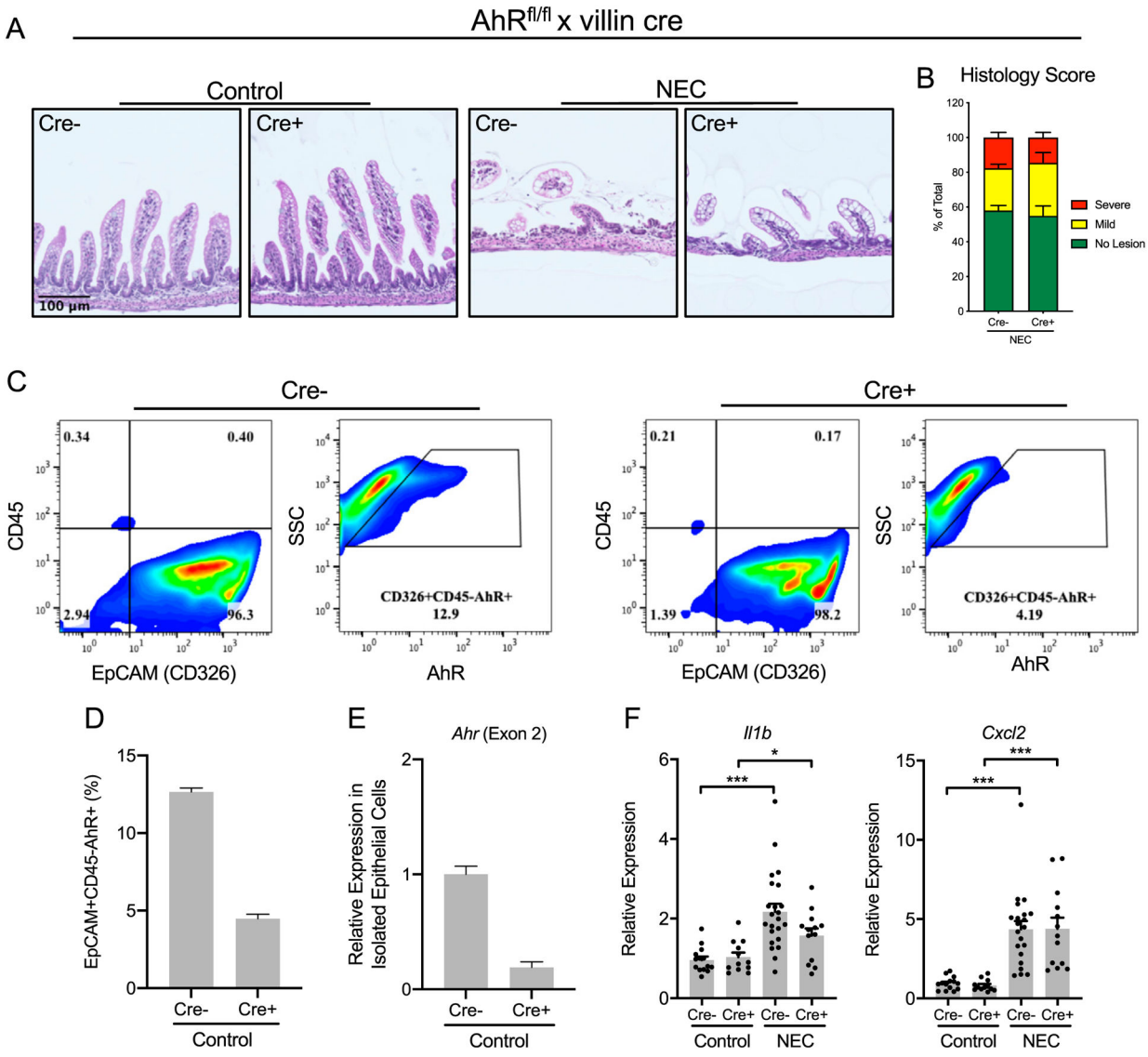

FIGURE 4. AhR signaling in IECs is dispensable in experimental NEC.

(**A**) Representative images of formalin-fixed, paraffin-embedded terminal ileum tissue sections from control and experimental pups were stained with H&E. (**B**) Tissue sections were used to quantify differences in histology scores in experimental pups with and without IEC-specific knockout without a significant difference in the proportion of lesions on NEC tissue sections. (**C** and **D**) Small intestine epithelial cells were isolated from $AhR^{\Delta IEC}$ pups ($n = 2$) and cre-negative littermates ($n = 2$) and stained with anti-EpCAM (anti-CD326) and anti-CD45, confirming positive isolation of epithelial cells and exclusion of lymphocytes. Flow cytometric analysis of isolated small IECs from cre-negative mice demonstrated a significantly increased percentage of AhR from $EpCAM^{+}CD45^{-}$ cells when compared with $AhR^{\Delta IEC}$ mice, confirming epithelial cell-specific knockout of AhR. (**E**) qRT-PCR reveals significantly reduced mRNA expression of *Ahr* (Exon 2) in the isolated epithelial cells from $AhR^{\Delta IEC}$ pups, confirming AhR-specific deletion in the IECs. (**F**) $AhR^{\Delta IEC}$ pups exhibited a similar susceptibility to experimental NEC compared with their cre-negative littermates,

without a significant difference in proinflammatory cytokine expression between the experimental NEC groups. *$p < 0.05$, ***$p < 0.0001$ by Mann-Whitney U test.

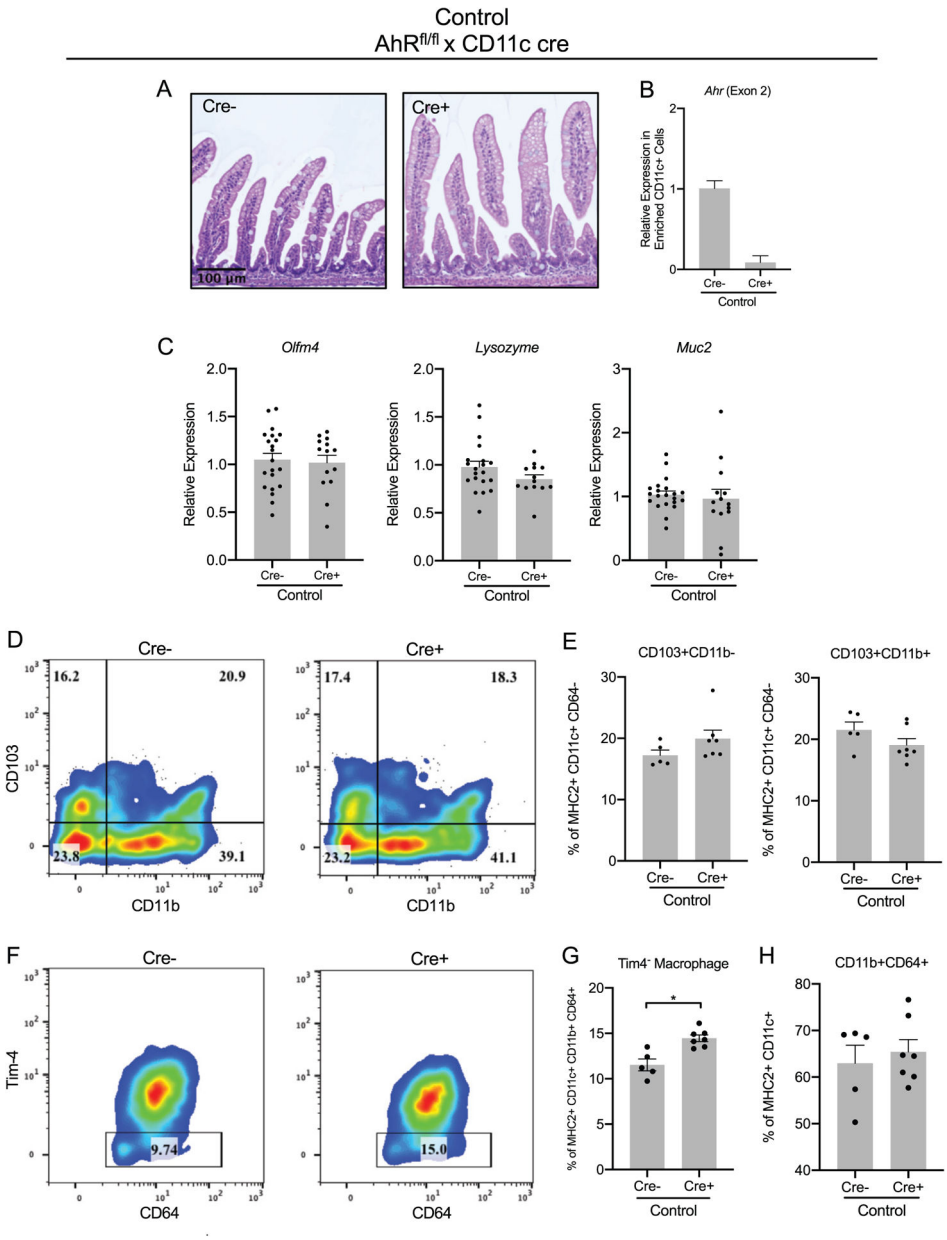

FIGURE 5. AhR signaling in CD11c$^+$ immune cells is not induced during homeostasis.

(**A**) Representative images of formalin-fixed, paraffin-embedded terminal ileum tissue sections from mice with CD11c$^+$ immune cell-specific knockout and cre-negative littermates during homeostasis were stained with H&E. (**B**) qRT-PCR analysis of enriched CD11c$^+$ cells **(continued)** from the small intestine lamina propria from AhR$^{\Delta CD11c}$ pups ($n = 2$) and wild-type littermates ($n = 2$) reveals significantly reduced mRNA expression of *Ahr* (Exon 2) in AhR$^{\Delta CD11c}$ pups, confirming AhR-specific deletion in the CD11c$^+$ immune cells. (**C**) Small intestine gene expression of IEC markers *Olfm4*, *Lysozyme*, and *Muc2* were analyzed by qRT-PCR and demonstrated no change in the expression in the AhR$^{\Delta CD11c}$ pups or their cre-negative littermates. (**D** and **E**) Flow cytometric analysis demonstrated no significant change in the abundance of CD103$^+$CD11b$^-$ and CD103$^+$CD11b$^+$ DCs in cre-negative and

$AhR^{\Delta CD11c}$ mice during steady state. (**F** and **G**) The Tim-4^{-} monocyte–dependent subset of macrophages in the small intestine lamina propria were increased in $AhR^{\Delta CD11c}$ pups compared with cre-negative pups, whereas (**H**) there was no difference in $CD11b^{+}CD64^{+}$ macrophages in cre-negative mice and $AhR^{\Delta CD11c}$ mice during the homeostatic state. Data represent mean ± SEM from three independent experiments. *$p < 0.05$, by Mann-Whitney U test.

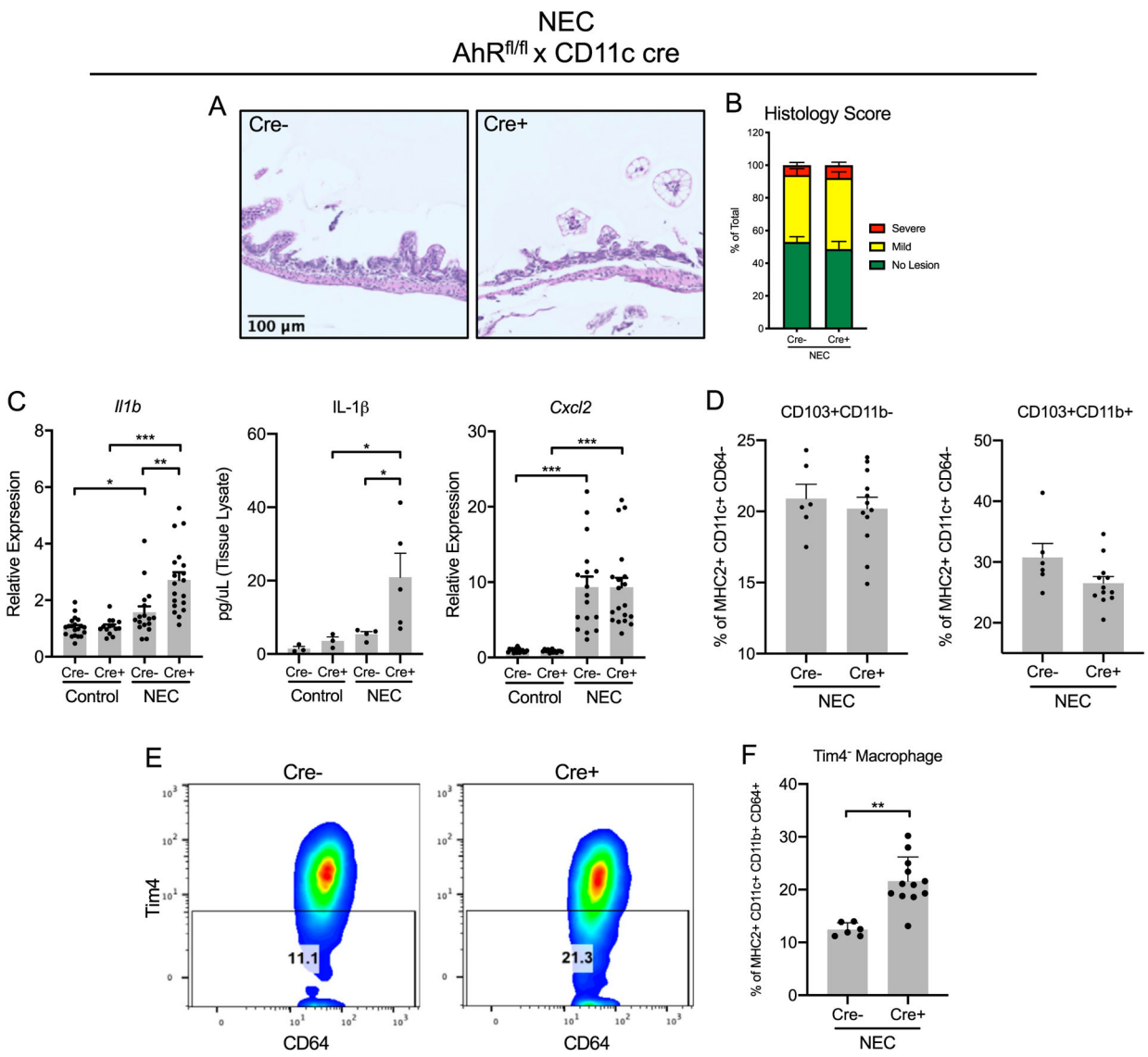

FIGURE 6. AhR signaling in CD11c$^+$ immune cells impacts the severity of inflammation during NEC.

(**A**) Representative images of formalin-fixed, paraffin-embedded terminal ileum tissue sections stained with H&E are shown. (**B**) Tissue sections were used to quantify differences in histology scores in experimental pups with and without CD11c$^+$ immune cell–specific knockout with no significant difference in the proportion of lesions on NEC tissue sections. (**C**) Relative expression of proinflammatory markers *Il1b* (left), quantitated by IL-1β protein concentration (middle), and *Cxcl2* (right) in the small intestine were determined by qRT-PCR. (**D**) Flow cytometric analysis revealed no significant change in the abundance of CD103$^+$CD11b$^-$ or CD103$^+$CD11b$^+$ DCs in cre-negative and AhR$^{\Delta CD11c}$ mice during NEC. (**E** and **F**) Increased Tim-4$^-$ monocyte-dependent subset of macrophages in the small intestine lamina propria in AhR$^{\Delta CD11c}$ pups was observed during NEC. Data represent mean

± SEM from three independent experiments. *$p < 0.05$, **$p < 0.005$, ***$p < 0.0001$ by Mann-Whitney U test.

TABLE I.

Primers for qRT-PCR analysis of gene expression

Gene	Species	Forward Primer	Reverse Primer	Amplicon Size (bp)
RPLO	Mouse/human	5′-GGCGACCTGGAAGTCCAACT-3′	5′-CCATCAGCACCACAGCCTTC-3′	143
AhR	Human	5′-TCCTTGGCTCTGAACTCAAGCTGT-3′	5′-GCTGTGGACAATTGAAAGGCACGA-3′	190
Ahr	Mouse	5′-ATGTCCATGTATCAGTGCCAG-3′	5′-CTGCTCAAGTCGGACGAATAG-3′	149
Ahr (Exon 2)	Mouse	5′-GAGACCGGCTGAACACAGAG-3′	5′-AAGAAGCTCTTGGCCCTCAG-3′	130
CYP1A1	Human	5′-GGCCACATCCGGGACATCACAGA-3′	5′-TGGGGATGGTGAAGGGGACGAA-3′	337
Cyp1a1	Mouse	5′-GACCCTTACAAGTATTTGGTCGT-3′	5′-GGTATCCAGAGCCAGTAACCT-3′	145
Cxcl2	Mouse	5′-CCAGACAGAAGTCATAGCCACT-3′	5′-GGCACATCAGGTACGATCCA-3′	217
Foxp3	Mouse	5′-ATTGAGGGTGGGTGTCAGGA-3′	5′-GTTCTTGTCAGAGGCAGGCT-3′	158
Fut2	Mouse	5′-CAGAAGAGCCATGGCGAGTG-3′	5′-CGTTGCTGGAGGTGGATGAT-3′	102
Ifng	Mouse	5′-AGGCCATCAGCAACAACATAAGCG-3′	5′-TGGGTTGTTGACCTCAAACTTGGC-3′	119
Il1b	Mouse	5′-AGTGTGGATCCCAAGCAATACCCA-3′	5′-TGTCCTGACCACTGTTGTTTCCCA-3′	175
Il6	Mouse	5′-GCCTTCTTGGGACTGATGCT-3′	5′-TGCCATTGCACAACTCTTTTC-3′	181
Il10	Mouse	5′-GCCTTATCGGAAATGATCCA-3′	5′-TCCTGAGGGTCTTCAGCTTC-3′	118
Il17a	Mouse	5′-ACTACCTCAACCGTTCCACG-3′	5′-TTCCCTCCGCATTGACACAG-3′	120
Il22	Mouse	5′-CGACCAGAACATCCAGAAGAA-3′	5′-GAGACATAAACAGCAGGTCCA-3′	110
Lcn2	Mouse	5′-GACTTCCGGAGCGATCAGTT-3′	5′-CTGTACCTGAGGATACCTGTGC-3′	258
Lysozyme	Mouse	5′-AAGCTGGCTGACTGGGTGTGTTTA-3′	5′-CACTGCAATTGATCCCACAGGCAT-3′	178
Muc2	Mouse	5′-TAGTGGAGATTGTGCCGCTGAAGT-3′	5′-AGAGCCCATCGAAGGTGACAAAGT-3′	168
Marco	Mouse	5′-CCAGGACTTTCAGGTGCCAA-3′	5′-TGGCCAGAAGACCCTTTCAT-3′	278
Olfm4	Mouse	5′-AAAGCTGTTAGGAGCAGCTGGAAG-3′	5′-TCACAGAAGGAGCGCTGATGTTCA-3′	140
Reg3g	Mouse	5′-GTACCCTGTCAAGAGCCTCA-3′	5′-TGTGGGGAGAATGTTCCCTT-3′	182
Tnf	Mouse	5′-TTCCGAATTCACTGGAGCCTCGAA-3′	5′-TGCACCTCAGGGAAGAATCTGGAA-3′	144